

Photon structure function and optimized perturbation theories

Hisao Nakkagawa

Institute for Natural Science, Nara University, 1230 Horai-cho, Nara 631, Japan

A. Niégawa and Hiroshi Yokota

Department of Physics, Osaka City University, Sumiyoshi-ku, Osaka 558, Japan

(Received 25 August 1986)

We study the consequences of Stevenson's optimized perturbation theory applied to the second-order QCD calculation of the moment of the photon structure function $F_{2\gamma}^n$. The singular $\ln n$ term present in the second-order coefficient in the conventional calculations based on the modified-minimal-subtraction and momentum-space-subtraction schemes is completely absorbed into the effective mass scale. Comparisons with other analyses are also made.

Perturbative QCD calculations of physical quantities depend explicitly on the procedure how we define the expansion parameter or the coupling constant¹⁻³ $a \equiv g_s^2/4\pi^2$. This ambiguity arises because we are free to prescribe how much of the finite parts of renormalization constants are left behind on taking the infinities away. Resolution of this renormalization-scheme (RS) dependence can be successfully carried out with the use of the optimized perturbation theory (OPT) proposed on the basis of the principle of minimal sensitivity by Stevenson.³

Within the second-order calculations, choosing the RS is equivalent to choosing the renormalization point μ . The response of the coupling a to a change of μ is given by the renormalization-group equation

$$\frac{\partial a}{\partial \ln \mu} = \beta(a) = ba^2(1 + ca + \dots), \tag{1}$$

where b and c are RS-independent constants. With the appropriate boundary condition³ we can integrate Eq. (1) in the form

$$\ln \frac{\mu}{\Lambda} = \int_0^a \frac{dx}{\beta(x)} - \int_0^\infty \frac{dx}{bx^2(1+cx)}, \tag{2}$$

whose second-order expression becomes

$$|b| \ln \frac{\mu}{\Lambda} = \frac{1}{a} + c \ln \left[\frac{ca}{1+ca} \right]. \tag{3}$$

Typical of the predictions of perturbative QCD are those for the structure functions of deep-inelastic scattering processes. The Mellin-transformed n th moment is calculated perturbatively in the form

$$F_2^n(Q^2) = A_n a^{d_n} (1 + r_n a + \dots), \tag{4}$$

where d_n is a RS-independent constant while r_n as well as a depends explicitly on the RS used in the calculation. The overall normalization A_n is, in general, *uncalculable* within the framework of perturbation theory, but is independent of scale μ .⁴

In order to get Eq. (4) we should factorize away the uncalculable "soft" part into parton distribution functions,

or the operator matrix elements A_n . This factorization procedure, which is interrelated with the renormalization of the operator matrix elements, again causes an ambiguity similar to the RS-dependent ambiguity.⁴⁻⁶ Therefore, generally speaking, the calculational scheme dependences of the perturbative results can be analyzed only if the RS dependence and the factorization-scheme (FS) dependence are taken into account simultaneously.⁷ However, there are quantities that are free of the FS dependences, e.g., in the present case the Q^2 dependence^{3,5} of the structure function F_2^n :

$$R_2^n(Q^2) \equiv \frac{1}{bd_n} \frac{d \ln F_2^n(Q^2)}{d \ln Q} = a(1 + h_n a + \dots), \tag{5}$$

where

$$h_n = c + r_n/d_n. \tag{6}$$

If we start with the perturbative calculation of R_2^n , then by applying the original single-scale OPT (Ref. 7) to the second-order approximation to $R_2^n(Q^2)$ we get the optimized solution⁸

$$[R_2^n(Q^2)]_{\text{OPT}} = a_{\text{OPT}} \frac{2 + ca_{\text{OPT}}}{2(1 + ca_{\text{OPT}})}, \tag{7}$$

$$|b| \ln \frac{Q}{\mu_{\text{OPT}}} = \rho_n + \frac{c}{2(1 + ca_{\text{OPT}})}, \tag{8}$$

where ρ_n is a RS invariant thus can be calculated in any scheme:

$$\rho_n = h_n - b \ln(Q/\mu). \tag{9}$$

Substituting Eq. (8) in Eq. (3) with μ and a replaced by μ_{OPT} and a_{OPT} , respectively, we get the determining equation for a_{OPT} :

$$|b| \ln \frac{Q}{\Lambda} = \rho_n + \frac{1}{a_{\text{OPT}}} + c \ln \left[\frac{ca_{\text{OPT}}}{1 + ca_{\text{OPT}}} \right] + \frac{c}{2(1 + ca_{\text{OPT}})}. \tag{10}$$

Having obtained $(R_2^n)_{\text{OPT}}$, we can evaluate $[F_2^n(Q^2)]_{\text{OPT}}$ at any Q^2 through a simple integration, once we know $F_2^n(Q^2)$ at some reference value of $Q^2 = Q_0^2$:

$$\ln[F_2^n(Q^2)]_{\text{OPT}} = \ln F_2^n(Q_0^2) + b d_n \int_{Q_0}^Q \frac{dQ'}{Q'} [R_2^n(Q'^2)]_{\text{OPT}}. \quad (11)$$

Thus we can apply the OPT to the perturbative analysis of the structure functions in two different ways:⁷ (i) applying the two-scale OPT (Refs. 4 and 5) to the structure function F_2^n itself that depends both on the RS and FS; (ii) applying the original single-scale OPT (Ref. 3) to the Q^2 dependence of F_2^n , Eq. (5), then integrate the result via Eq. (11) to get back the structure function.

In view of the above considerations the photon structure function $F_{2\gamma}^n$ shows a particular feature in its perturbative regime because the asymptotically dominant point-like contribution is free of the unknown parton distribution functions and can be calculated purely from QCD (Refs. 9 and 10). Namely, A_n (denoted explicitly as A_n^γ in the photonic case) in Eq. (4) belongs to the “hard” part in the sense that A_n^γ is, in contrast with the hadronic case, *calculable* in the leading-order perturbation calculation and is independent of RS. This fact means that, if we confine our interest in the asymptotically dominant contributions, the factorization of the photon structure function is carried out trivially or, in other words, there is no need to factorize the whole process into the “soft” and “hard” parts. Thus at first sight one may expect that the original single-scale OPT can be applied directly to the structure function $F_{2\gamma}^n$ itself and get the optimized solution. This is *not* the case³ simply because $d_n^\gamma = -1$ in Eq. (4).

If we employ the two-scale OPT, the above difficulty can be overcome and the optimized solution to the photon structure function is in fact obtained.¹¹ The purpose of the present note is to apply the alternative method or the single-scale OPT to the photon structure function and study the consequences of the result. As can be seen below, there are some differences between two optimization methods.

As explained above, in the single-scale OPT, the “optimized” $F_{2\gamma}^n(Q^2)$ can be obtained at any Q^2 through Eq. (11) provided that it is known at some reference value of $Q^2 = Q_0^2$. Remarkably enough, thanks to the asymptotic freedom, QCD predicts $F_{2\gamma}^n(Q^2)$ *exactly* at a special value of Q^2 , i.e., $Q^2 = \infty$. Namely, the leading-order coefficient A_n^γ is now exactly calculable, as stressed above. Substituting Eq. (7) in Eq. (11), changing the integration variable Q' to $a_{\text{OPT}}(Q')$ by the use of Eq. (10) and taking the limit $Q_0 \rightarrow \infty$, we get (hereafter we shall neglect the subscript OPT)

$$F_{2\gamma}^n(Q^2) = \frac{A_n^\gamma}{a} \exp \left[\frac{3}{4} \ln(1+ca) + \frac{6+5ca}{8(1+ca)^2} ca \right]. \quad (12)$$

This single-scale OPT solution is the main result in the present note.

In Fig. 1, the single-scale OPT result, Eq. (12), with four quark flavors is shown over the range $3 \leq n \leq 50$. We

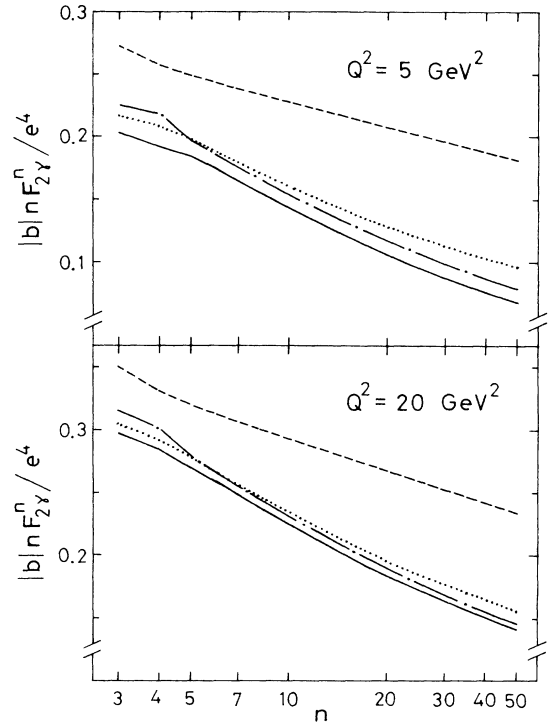


FIG. 1. Moments of the photon structure function $F_{2\gamma}^n$ in units of $e^4/|b|$, predicted by the leading-order QCD calculations (Ref. 9) (dashed curve), the second-order calculations in the $\overline{\text{MS}}$ scheme (Ref. 10) (dotted curve), the two-scale OPT calculations (Ref. 11) (dashed-dotted curve), and the single-scale OPT calculations Eq. (12) (solid curve). The predictions are for $\Lambda = 0.2$ GeV and four quark flavors. We have plotted n times the structure-function moments, for convenience.

have used the value of the scale parameter $\Lambda = \Lambda_{\overline{\text{MS}}} = 0.2$ GeV that corresponds³ to $\tilde{\Lambda} \simeq 0.224$ GeV for four quark flavors. For comparison, we also show the results for the leading-order calculations,⁹ for the second-order calculations in the modified minimal-subtraction ($\overline{\text{MS}}$) scheme,¹⁰ and for the two-scale OPT result.¹¹ Available experimental data are not accurate enough to discriminate one scheme from another. In the following we will discuss characteristic features of various calculations.

As seen from Fig. 1, both of the optimized solutions, i.e., the single- and the two-scale OPT results, share quite a similar n dependence. In fact, for $3 \leq n \leq 50$, their ratios are within the range 0.86–0.94 and 0.94–0.97 at $Q^2 = 5$ and 20 GeV², respectively.¹²

Two widely used conventional calculations, i.e., the $\overline{\text{MS}}$ calculations and the MOM (momentum-space subtraction scheme) calculations² (not shown in Fig. 1), also show similar n dependence between themselves. Their ratios are in the range¹³ 1.06–1.09 and 1.03–1.04 at $Q^2 = 5$ and 20 GeV², respectively. Note, however, that the two OPT results and the conventional calculations show quite different n dependences.

In order to study the behavior of the ordinary perturbation coefficients calculated in various schemes, we expand $F_{2\gamma}^n$ in the form of Eq. (4) with $d_n^\gamma = -1$:

TABLE I. The second-order to the leading-order ratio $r_n a(M(Q))$ for the original $\overline{\text{MS}}$ (Ref. 10) and for the two OPT calculations. The two-loop effective coupling constant in the $\overline{\text{MS}}$ scheme is calculated with $M=Q$ and $\Lambda_{\overline{\text{MS}}}=0.2$ GeV.

n	$r_n a(M(Q))$					
	$Q^2=5 \text{ GeV}^2$		$\overline{\text{MS}}$	$Q^2=20 \text{ GeV}^2$		$\overline{\text{MS}}$
	Single-scale OPT	Two-scale OPT		Single-scale OPT	Two-scale OPT	
3	0.439	-0.0735	-0.343	0.265	-0.0539	-0.276
5	0.443	-0.0174	-0.346	0.266	-0.0123	-0.278
10	0.565	0.0046	-0.414	0.302	0.0031	-0.332
15	0.681	0.0187	-0.454	0.329	0.0119	-0.365
20	0.788	0.0352	-0.479	0.349	0.0215	-0.385
25	0.890	0.0535	-0.497	0.364	0.0315	-0.400
30	0.989	0.0730	-0.511	0.377	0.0416	-0.411
35	1.087	0.0933	-0.522	0.388	0.0515	-0.419
40	1.184	0.1142	-0.531	0.398	0.0612	-0.427
45	1.282	0.1357	-0.538	0.406	0.0707	-0.433
50	1.382	0.1577	-0.545	0.414	0.0798	-0.438

$$F_{2\gamma}^n = \frac{A_n^\gamma}{a} (1 + r_n a + \dots), \quad (13)$$

where r_n as well as a depends on the scheme used, while A_n^γ does not. The single-scale OPT result, Eq. (12), gives

$$r_n(\text{single-scale OPT}) = \frac{3}{2}c, \quad (14)$$

whose n independence is a striking result about which we will discuss later. First let us study the consequences of the numerical analysis. In Table I we give the second-order to the leading-order ratio $r_n a$ for various calculations.¹⁴ Both of the OPT predict the second-order coefficients to be *always positive* (except for small n), in contrast with the original $\overline{\text{MS}}$ or MOM calculations in which the second-order coefficients are always negative. As can be seen from Table I, at $Q^2=5 \text{ GeV}^2$, the single-scale OPT predicts $r_n a$ to exceed unity at $n=31$ and then we cannot take the result for $n \geq 31$ seriously.

Second let us study the large- n behavior of the perturbation coefficient r_n . In the conventional calculations, e.g., in the $\overline{\text{MS}}$ schemes, r_n in Eq. (13) behaves⁸ as $\ln n$ for large n . In the single-scale OPT calculations, r_n is independent of n as noted above [see Eq. (14)]. This means that the $\ln n$ singularity present in r_n is completely absorbed into the optimized mass scale μ_{OPT} or the coupling constant a_{OPT} [see Eq. (8)] through the process of optimization. This is in a sharp contrast to the two-scale OPT result in which only a part of the $\ln n$ singularity is absorbed into the mass scale.^{8,11}

Finally we give a comment on the comparison between the photon and the hadron structure functions. We can

get two “optimized” solutions for the Q^2 dependence $R_{2\gamma}^n$ through the two OPT procedures. One result is Eq. (7) with Eq. (10) that is obtained through the direct application of the single-scale OPT to $R_{2\gamma}^n$, Eq. (5) with $d_n^\gamma = -1$. The other one is obtained as follows: first apply the two-scale OPT to the photon structure function $F_{2\gamma}^n$ itself; then, by using quantities thus optimized, evaluate $R_{2\gamma}^n$ directly.⁸ The difference between these “optimized” solutions can be shown to be of $O(a^3)$, which is just the order of the RS-dependent ambiguity. This result is to be contrasted with the hadronic structure-function case⁸ where the difference between the two OPT results for R_2^n is of $O(a^5)$, two orders higher than expected. This difference is not surprising from the following observation: Although the single-scale optimization of R_n works in a same manner for the photonic and hadronic cases, the same is not true for the two-scale optimizations. The photonic case is considerably more complicated and it is not just like the nonsinglet hadronic case with $d_n \rightarrow d_n^\gamma = -1$.

In conclusion two OPT results for the photon structure function share many desirable features. Furthermore, their perturbative coefficients have similar n dependence and their ratio is rather close to unity. For this reason it seems to be difficult to discriminate them experimentally. However, the n dependence of the two OPT results is quite different from those of the conventional calculations such as $\overline{\text{MS}}$ and MOM calculations, especially in the small- n region, and may be compared with experiment rather easily.

¹See, e.g., D. W. Duke and R. G. Roberts, Phys. Rep. **120**, 275 (1985), and references therein.

²W. Celmaster and R. J. Gonsalves, Phys. Rev. Lett. **42**, 1435 (1979); Phys. Rev. D **20**, 1420 (1979); W. Celmaster and D. Sivers, *ibid.* **23**, 227 (1981).

³P. M. Stevenson, Phys. Lett. **100B**, 61 (1981); Phys. Rev. D **23**, 2916 (1981).

⁴H. Nakkagawa and A. Niégawa, Phys. Lett. **119B**, 415 (1982); Prog. Theor. Phys. **70**, 511 (1983); **71**, 339 (1984); **71**, 816 (1984).

⁵H. D. Politzer, Nucl. Phys. **B194**, 493 (1982); P. M. Stevenson and H. D. Politzer, *ibid.* **B277**, 758 (1986).

⁶W. Celmaster and D. Sivers, Ann. Phys. (N.Y.) **143**, 1 (1982).

⁷The two-scale OPT has been invented by Politzer (Ref. 5) and

by us (Ref. 4) to resolve these two ambiguities simultaneously, and successfully applied to the hadronic structure function. In the two-scale OPT two mass scales enter the stage, one of which specifies the renormalization scale and the other the factorization scale. To discriminate this two-scale OPT from the original OPT (Ref. 3), we refer to the latter as the single-scale OPT, hereafter.

⁸H. Nakkagawa, A. Niégawa, and H. Yokota, *Phys. Rev. D* **34**, 244 (1986).

⁹E. Witten, *Nucl. Phys.* **B120**, 189 (1977).

¹⁰W. A. Bardeen and A. J. Buras, *Phys. Rev. D* **20**, 166 (1979).

¹¹H. Nakkagawa, A. Niégawa, and H. Yokota, *Phys. Rev. D* **33**, 46 (1986).

¹²Especially at $Q^2=20 \text{ GeV}^2$ this ratio takes an almost constant value of 0.94 over the range $5 \leq n \leq 50$.

¹³The quoted values correspond to the case $\Lambda_{\text{MOM}}=1.79\Lambda_{\overline{\text{MS}}}$ which comes from the definition of the coupling constant via the triple-gluon vertex with the use of the Feynman gauge (Ref. 2). If we instead use $\Lambda_{\text{MOM}}=2.73\Lambda_{\overline{\text{MS}}}$ (corresponding to define the coupling constant via the ghost-gluon vertex with the Feynman gauge), we have 1.11–1.18 and 1.06–1.07, respectively.

¹⁴The coupling constant in the $\overline{\text{MS}}$ scheme takes the value 0.0766 and 0.0615 at $Q^2=5$ and 20 GeV^2 , respectively. In Ref. 11, there were mistakes in the numerical estimates of the $\overline{\text{MS}}$ results, and accordingly the corresponding $\overline{\text{MS}}$ column in Table III should be replaced with that of Table I in this paper. The observations and conclusion made in Ref. 11 based on Table III are, however, not changed at all by this modification.